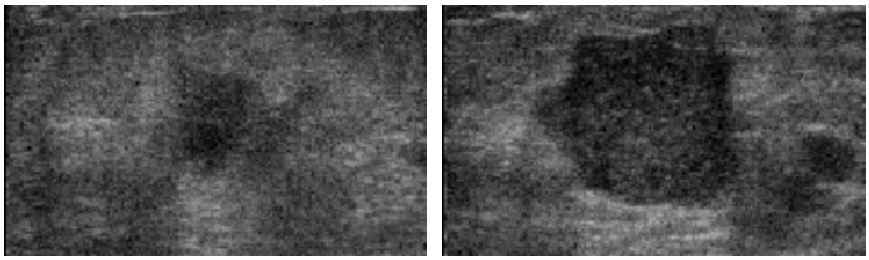

**Figure 1.** Example of two desired ultrasound images of a breast lesion for which our proposed methodology was developed.


**Figure 2.** (a) Level set bounding the search space. (b) Initial function with zero level set as the contour presented.

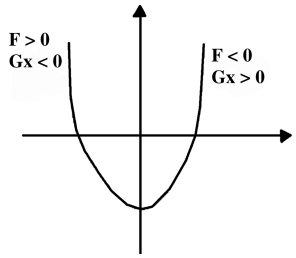


**Figure 3.** Sign of the speed function.

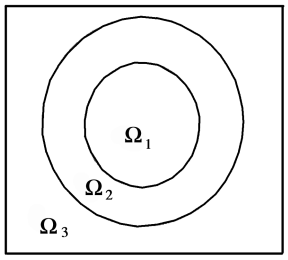


**Figure 4.** Support of step function given by Eq. (28) with $a_i = 1$, $a_2 = -1$ and $a_3 = 1$.

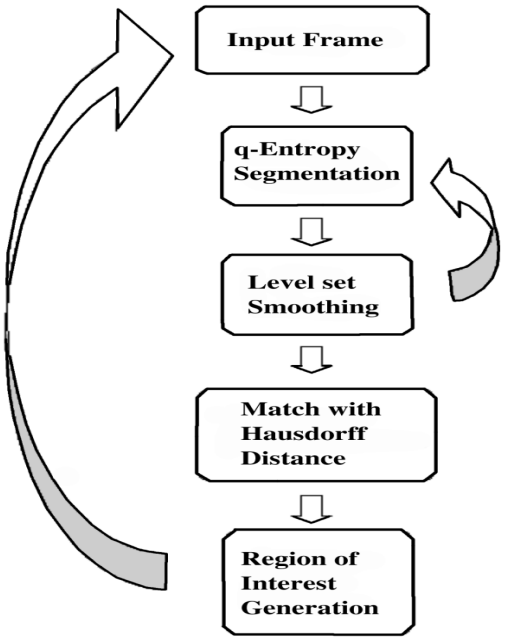


**Figure 5.** Schematic view of the proposed HTLS algorithm. The initial user-defined ROI is not shown.

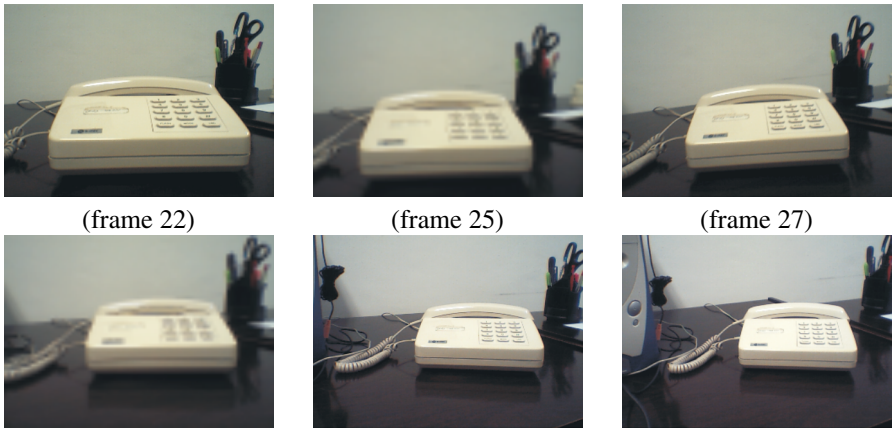


**Figure 6.** Sequence of images from an office table with slight camera movement, changes in illumination, and a heterogeneous background.


**Figure 7.** Four sequences of images from the Columbia database. Each row is an object sequence. This database has several object viewers and zoom, which is suitable for evaluating the performance of our proposed algorithm.

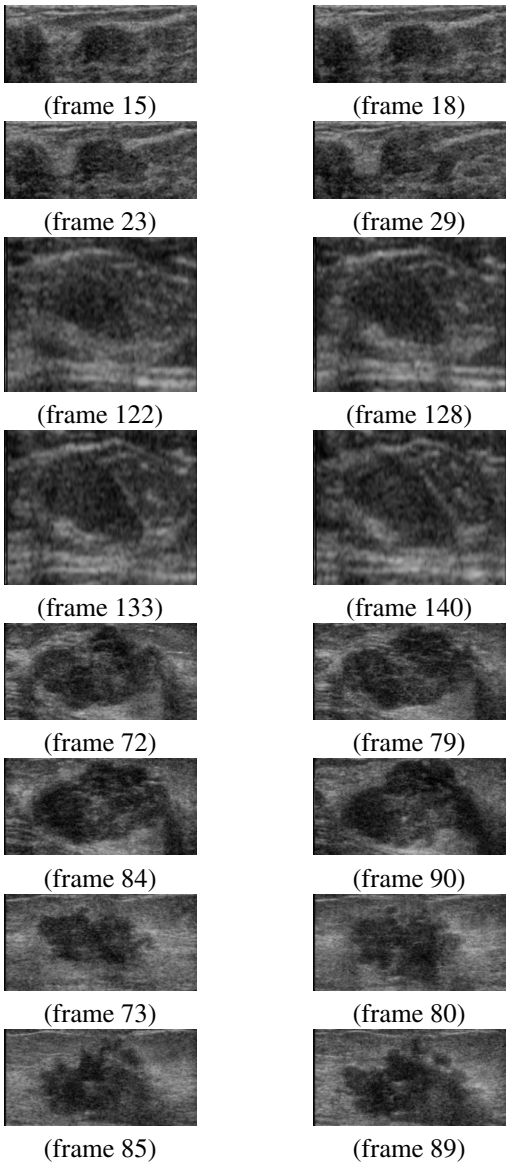


**Figure 8.** Four sequences of images from the Columbia database. Each row is an object sequence. This database has several object viewers and zoom, which is suitable for evaluating the performance of our proposed algorithm.

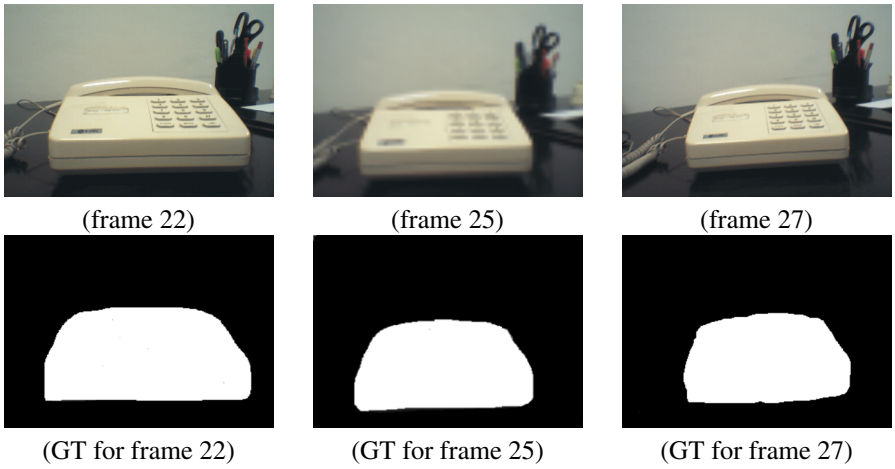


**Figure 9.** Three images (top row) from the first class and their corresponding manually traced ground truth (bottom row). GT = ground truth.

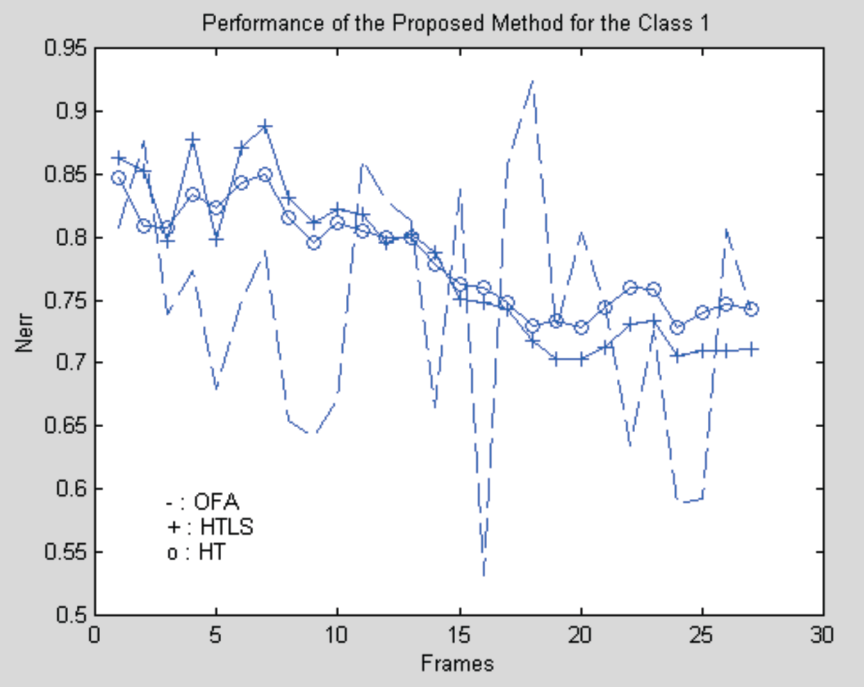


**Figure 10.** Performance evaluation of the HTLS algorithm as a function of frames for the first class sequence. "o" represents the HTLS performance; "+" represents HT algorithm performance; "–" represents OFA algorithm performance.

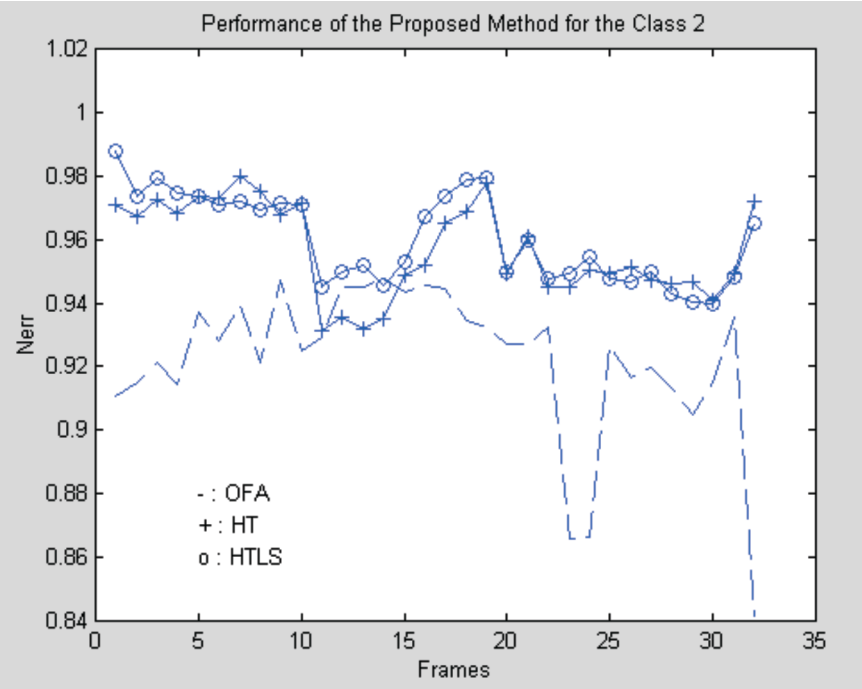


**Figure 11.** Performance of the HTLS algorithm as a function of frames for the class 2 sequence. "o" represents HTLS performance; "+" represents HT performance; "–" represents OFA performance.

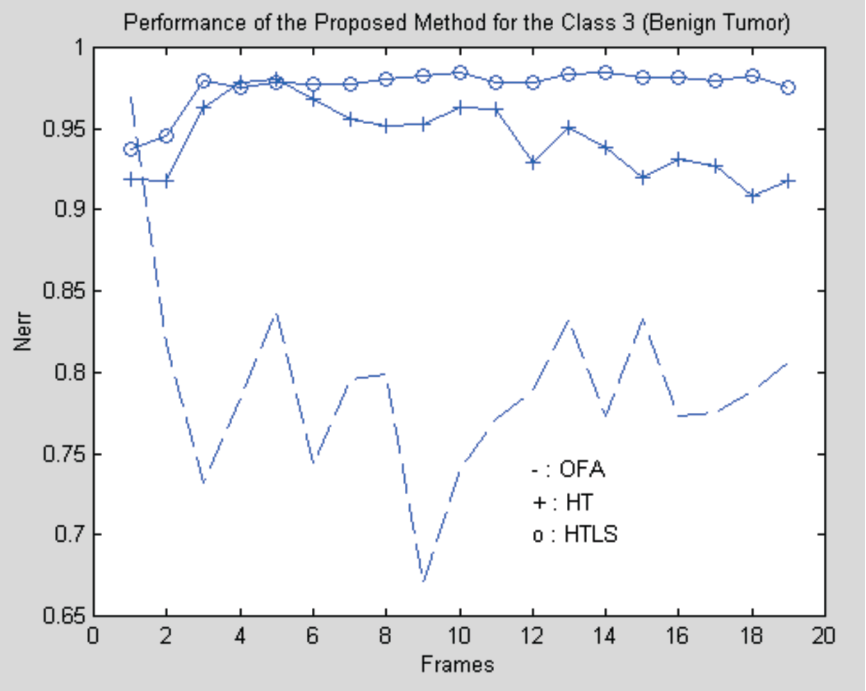


**Figure 12.** Performance of the HTLS algorithm for class 3 images (benign tumor). "o" represents HTLS performance; "+" represents HT performance; "–" represents OFA performance.

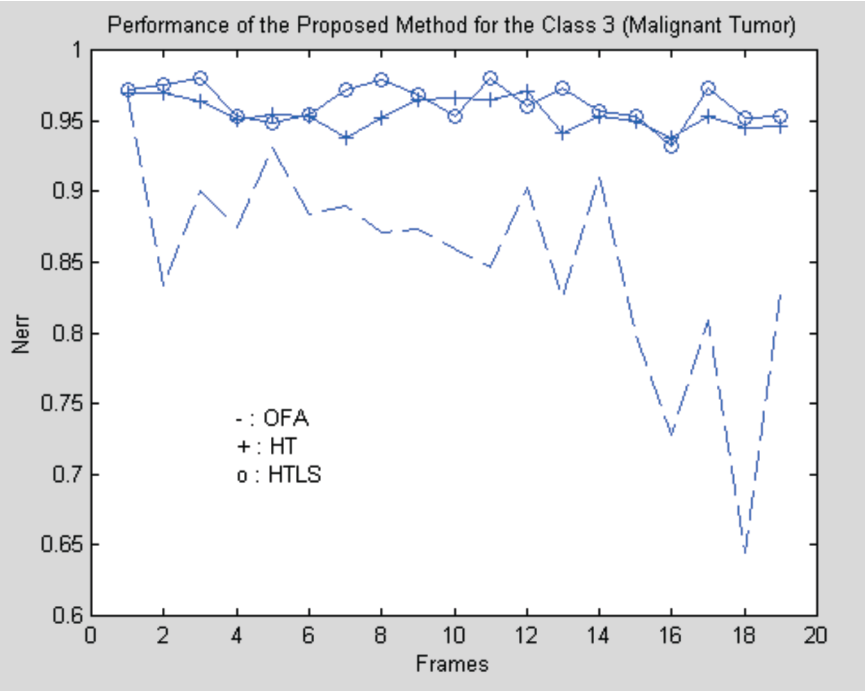


**Figure 13.** Performance of the HTLS algorithm with class 3 images (malignant tumor). "o" represents HTLS performance; "+" represents HT performance; "–" represents OFA performance.

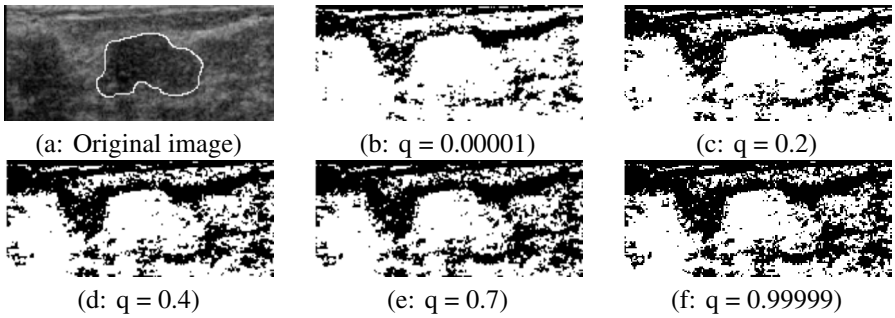


**Figure 14.** Mammographic image and five segmentations with different $q$ values: (a) original image; (b)–(f) segmentation for $q$ = (0.00001, 0.2, 0.4, 0.7, 0.9999). Intuitively, in this case, as $q$ approaches 1, the images seem to become well segmented.

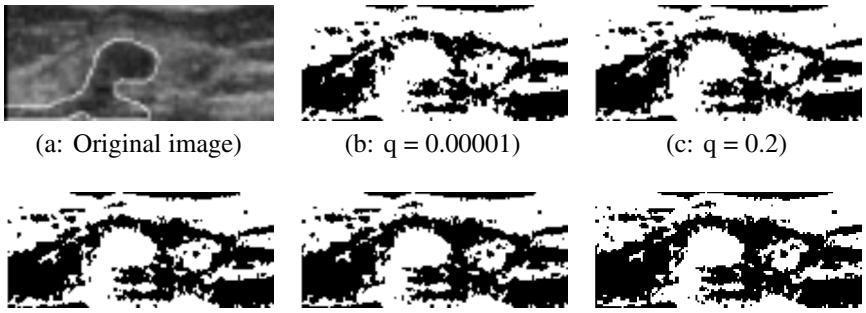


**Figure 15.** Mammographic image and 5 segmentation with different $q$ values: (a) original image; (b)–(f) segmentation for $q = (0.00001, 0.2, 0.4, 0.9999)$. In this case, as $q$ approaches 0, the images seem to become well segmented.

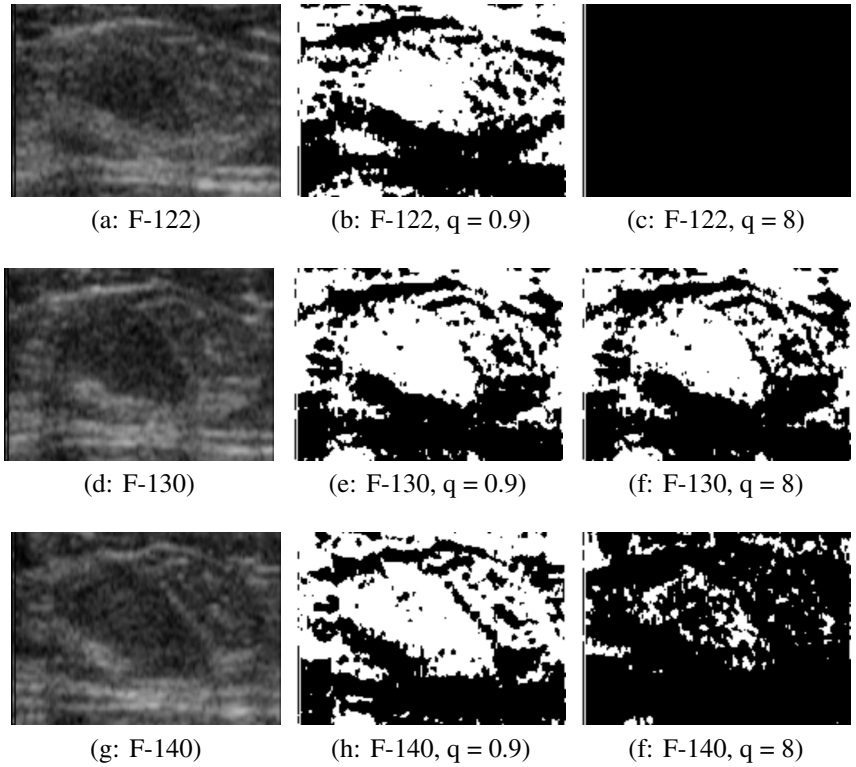


**Figure 16.** Frame sequence (frames 122, 130, and 140) of ultrasound images. Each row corresponds to a frame and two segmentations for $q = 0.9999$ and $q = 8$. For different frames we need different $q$ values to achieve a good segmentation.

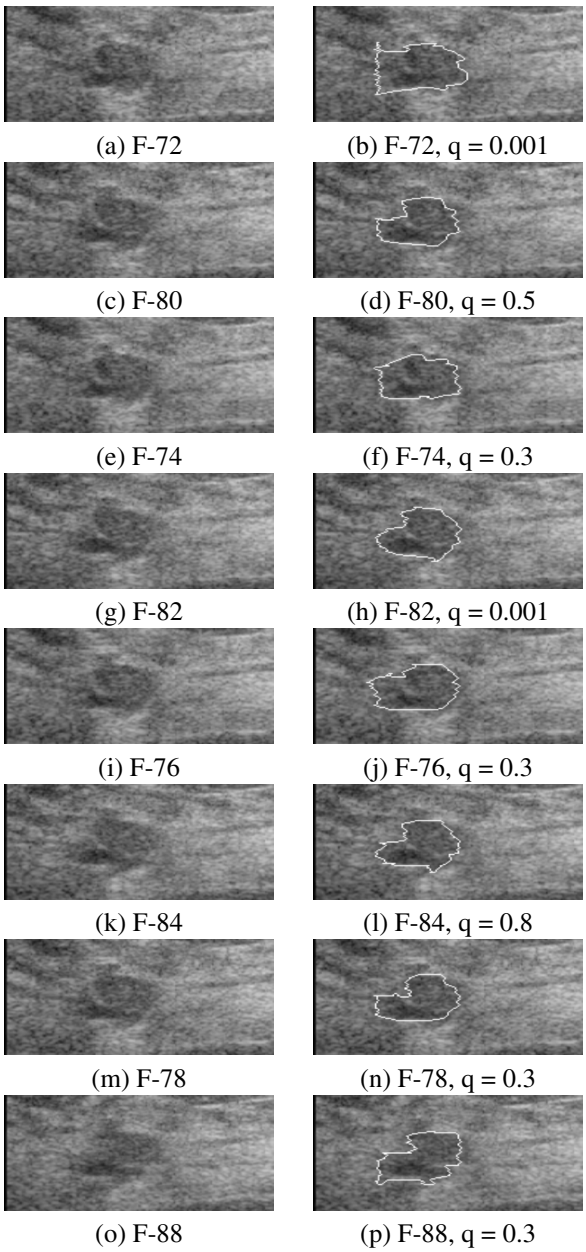


**Figure 17.** Eight images from a frame sequence of a benign tumor. The left column includes the original images; the right column presents their corresponding achieved boundary with their respective best $q$ values (indicated below each image).

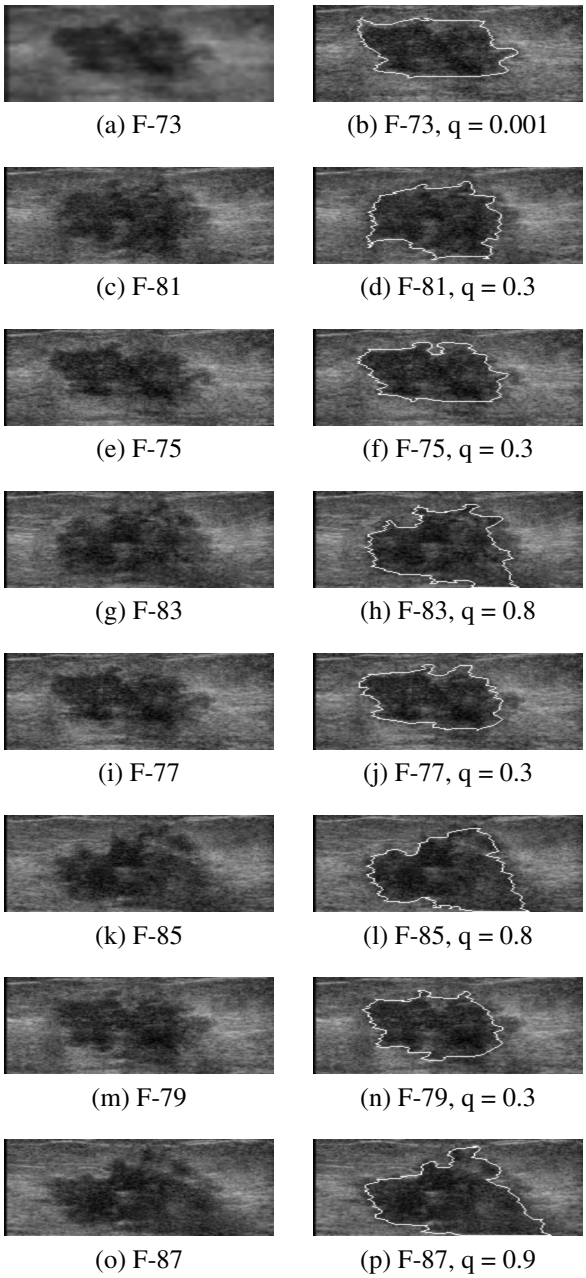


**Figure 18.** Eight images from a frame sequence of a malignant tumor. The left column includes the original images; on the right are their corresponding achieved boundary, with their respective best $q$ values shown below.